# Nuclear dynamics during the N 1*s* autoionization of physisorbed $N_2$

C. Keller and M. Stichler
*Physik-Department E20, Technische Universität München, 85747 Garching, Germany*

G. Comelli, F. Esch, and S. Lizzit
*ELETTRA, Sincrotrone Trieste S.C.P.A., 34012 Basovizza, Italy*

Z. W. Gortel
*Department of Physics, University of Alberta, Edmonton, Alberta, Canada T6G 2J1*

W. Wurth and D. Menzel
*Physik-Department E20, Technische Universität München, 85747 Garching, Germany*

(Received 15 June 1999)

We demonstrate that even for adsorbed molecules, the vibrational fine structure of resonant core hole decay channels after narrow-band excitation can show a dependence on the variation of the primary excitation energy as known from isolated molecules. Despite several adsorption-induced broadening mechanisms, the so-called detuning effect can be observed in the autoionization of a $N_2$ monolayer physisorbed on Xe/Ru(001) for the $1\pi_u^{-1}$ final state of participant decay, in good agreement with theoretical predictions and observations for isolated $N_2$. However, contrary to the corresponding decay channel of isolated $N_2$ and to the theoretical predictions for it, the decay into the $3\sigma_g^{-1}$ final state shows clearly different behavior much closer to that of normal Auger decay. This is partly due to final-state broadening. [S0163-1829(99)07947-3]

## I. INTRODUCTION

Since third-generation synchrotron sources with high resolution and high flux monochromators in the soft-x-ray regime have become available, the investigation of electronic decay processes after resonant core-hole excitation has attracted considerable interest. The resonant excitation of a core electron to a bound state by resonant photon absorption results in a neutral core-excited state which decays dominantly via autoionization (resonant Auger transition) for light elements. If the bandwidth of the resonantly exciting radiation is narrower than the natural core-hole lifetime width $\Gamma$, excitation and decay have to be described as a coherent one-step process.[1,2] For isolated atoms the subsequent decay channels after narrow-band core excitation show two distinct characteristics of the so-called Auger resonant Raman (ARR) effect: the kinetic energies track the excitation energy (linear dispersion),[3,4] and the linewidth of the decay spectra is determined by the bandwidth of the excitation energy[5] (line-narrowing effect). These effects are a consequence of energy conservation for the coherent one-step process. They were first observed in the x-ray range for deep core-hole states with rather short lifetimes by Brown *et al.*[6] in 1980.

Up until recently, the bulk of published ARR studies in the soft-x-ray regime concerned isolated noble-gas atoms.[7–9] ARR spectroscopy of isolated molecules is more complicated, but also much more informative because of the influences of nuclear dynamics during core-hole decay, including lifetime-vibrational interference effects, in resonantly excited decay spectra.[10,11] The lifetime broadening of the core-excited state for low-*Z* atoms is typically of the same order as the vibrational spacing of dominant vibrations in small molecules consisting of these atoms.

Experimental studies under ARR excitation conditions of small diatomic molecules such as CO,[12–14] $N_2$,[15,16] and HCl (Refs. 17 and 18), have been published only recently. In particular, the nuclear dynamics and the dissociation, which take place within a time scale comparable to the lifetime $\hbar/\Gamma$ of the resonant core-hole excitation, are of interest. Meanwhile, time-independent as well as time-dependent unified theoretical treatments of molecular resonant Auger processes and connected photodissociation have been formulated.[19–23]

In the molecular resonant Auger process, the initial wave packet in the ground state is excited to the intermediate core-excited state through interaction with the electromagnetic field. While nuclear wave packets in the intermediate state are added continuously by the excitation with phases controlled by the exciting radiation frequency, they propagate on the intermediate state potential-energy surface, interfering with each other, and simultaneously decay to the final electronic state by emitting resonant Auger electrons. The decayed components propagate on the potential-energy surfaces of the corresponding final states and again may interfere with new contributions added continuously from the decaying state.

The vibrational structure of such resonant Auger decay spectra depends strongly on the exact photon frequency. For building up the vibrational fine structure, a ''spectrum formation time,'' $\tau_C$, is needed that can be interpreted as an effective propagation time of the wave packet in the core-excited state, during which the nuclear wave packet interacts with the core-excited potential-energy surface; for on-resonance excitation it is equal to the core-hole lifetime $\hbar/\Gamma$. Detuning of the excitation energy from the maximum of the resonance to lower or higher photon energies shortens the spectrum formation time $\tau_C$, because destructive interference between parts of the nuclear wave packet created earlier and later in the core-excited state becomes increasingly

 ©1999 The American Physical Society

important.[22,23] Using the detuning variable $\Omega$ the energetic difference between the absorption resonance and the center of the excitation energy, the spectrum formation time $\tau_C$ is given as $\tau_C = \hbar/2[\Omega^2 + (\Gamma/2)^2]^{1/2}$ (Refs. 24–26). Consequently $\tau_C$ depends strongly on the excitation energy and is drastically shortened by detuning. An analogous effect is the change of the rotational fine structure and the decrease of the scattering time observed already 25 years ago in normal resonant Raman scattering of isolated diatomic molecules when the laser frequency was detuned from a discrete electronic resonance.[27,28] A spectacular example in the context of core excitations is the observation by Skytt *et al.*[24] that the symmetry breaking in resonant inelastic x-ray scattering of $CO_2$ is quenched when the excitation energy is detuned from the nominal resonance energy.

The dependence of the vibrational structure of resonant Auger decay channels on the excitation energy caused by the so-called detuning effect was first experimentally proven for the C 1*s* autoionization of isolated CO by Sundin *et al.*[14] For excitation on the maximum of the resonance ($\Omega = 0; \tau_C = \hbar/\Gamma$) and a core-hole lifetime not too short compared with nuclear motion, the nuclear wave packet propagates sufficiently long on the potential-energy surface of the *core-excited* state to probe in detail its vibrational structure. When the exciting photon energy is detuned below the resonance ($\Omega > 0$), the vibrational fine structure is changed as a result of the decreased spectrum formation time $\tau_C$ in accordance with the formula given above, because now the nuclear wave packet has effectively less time and therefore probes a more limited part of the potential-energy surface of the core-excited state. For large values of the detuning variable $\Omega$, the spectrum formation time $\tau_C$ becomes so short that the nuclear wave packet of the ground state is effectively placed directly on the potential-energy surface of the electronic final state as in the normal photoemission process. In this case the vibrational profile reduces to a single line corresponding to the vibrational ground state $v = 0$ of the electronic final state, if the potential-energy surfaces of the *ground* and the *final* states are nearly identical. This dramatic detuning phenomenon has been called vibrational collapse effect.[14,26] On the other hand, if the potential-energy curves of the *intermediate* and the *final* state are similar and different from that of the ground state, the spectrum *on* resonance consists mainly of *one* vibrational line, but with increasing detuning goes over to increasing contributions from several vibrational levels of the electronic final state. Examples for both behaviors were predicted[23] for the $3\sigma_g^{-1}$ and the $1\pi_g^{-1}$ participant lines, respectively, of isolated $N_2$, for which it has been reported recently.[16]

Obviously this picture applies to the case of an isolated molecule when no coupling to other degrees of freedom is possible. If such coupling becomes possible by condensing or adsorbing an isolated system on a surface, this picture can break down for part or most of the excitations depending on the strength of the coupling between adsorbate and substrate, as has been shown recently.[29–32] It is an interesting question to examine how much of the detuning effects survive, if the coupling is made very weak. In the present study we have therefore looked for similarities and/or changes in the core excitation-induced nuclear dynamics of weakly coupled molecules on a surface. As a model system we have chosen physisorbed $N_2$ molecules decoupled from the underlying Ru(001) substrate by the preadsorption of a monoatomic Xe spacer layer.[33]

In the following we first discuss briefly the possible effects incurred by adsorption, and some experimental details. We then give the results of our experiments, and discuss them in connection with calculations based on the explicitly time-dependent theory described earlier.[23]

## II. THE ADSORBATE CASE

In the case of adsorbed systems there are certain peculiarities of excitation-decay processes that have to be considered. If the resonance state, into which the core electron is excited, lies energetically above the Fermi level of the substrate, the resonant Auger spectrum can consist of two types of decay channels, coherent resonant Auger Raman type *and* incoherent normal Auger type.[29–32] Because of the coupling between the adsorbate and the substrate, the coherent resonant decay of the core-excited state is in competition with charge transfer of the excited electron into the substrate before the core-hole decay. The coherence is lost by the charge-transfer process, so that the Auger decay channels of the ionized adsorbed system show normal, incoherent Auger behavior; the final states contain two valence holes. For the resonant core-hole decay channels in which the excited electron stays localized for the core-hole lifetime, coherent Auger Raman behavior is observed; the final states contain one valence hole or two holes and one electron. Strongly coupled chemisorbed systems show very fast charge transfer after resonant core excitation, so that the coherent Auger Raman decay channels are almost completely suppressed.[34] However, if the resonance state into which the core electron is excited is located energetically below the Fermi level of the substrate, the core-excited state can decay only via coherent resonant Auger Raman channels independent of coupling strength, simply for energetic reasons. This is the case for the system investigated here, $N_2$ on a complete monolayer of Xe on Ru(001).

For isolated systems the lifetime of a final valence hole state reached after the autoionization process is in most cases infinite on the time scale of the core-hole decay process ($10^{-9}$ sec or more, as compared to some $10^{-15}$ sec). Hence, for isolated systems the line shape of resonant Auger decay channels excited with subnatural linewidth radiation is determined solely by the experimental resolution. Because adsorption induces additional line broadening mechanisms in the final state, this so-called line narrowing effect is usually not observed for adsorbed systems. There are several possible reasons for adsorbate-induced line broadening. The valence hole final state of an adsorbed system can be neutralized by the interaction with the substrate or with the next neighbor. Thus the valence hole can effectively delocalize into the substrate or within the adsorbed layer. Delocalization within the adsorbate layer can occur in different ways. If the adsorbate has a periodic ordered structure, the electronic states possess a two-dimensional band structure.[35,36] For ordered molecular physisorbates, a two-dimensional band structure in the valence region can also be found, albeit with a smaller bandwidth.[37] For poorly ordered physisorbed systems, the coupling between the neighboring molecules can

still be of the same order as for well-ordered systems. Therefore, even if the adsorbate does not show perfect long-range order, as is the case for the $N_2$ physisorbate discussed here,[38] the valence hole can delocalize via hopping to the next neighbors.[33] The coupling, and thus the probability for the delocalization process, is strongest for the outer valence orbitals, because their orbital overlap is highest. This introduces a limitation on the lifetime of valence hole states—or equivalently on the definition of the final-state energy—so that the resonant Auger decay channels of an adsorbate appear always broadened.

For physisorbed systems which are not perfectly ordered, an additional contribution to broadening will be inhomogeneous. When a hole state is created within a physisorbate, the hole is screened by polarization of the next neighbors. The corresponding energy will vary, because within the partly disordered physisorbed layer the effective number of the surrounding atoms or molecules and their distances varies. Despite very high experimental resolution, the measured resonant Auger decay channels of a less than perfectly ordered physisorbate will then be inhomogeneously broadened. These adsorption-induced inhomogeneous as well as homogeneous broadening mechanisms limit the resolution of adsorbate autoionization measurements.[34]

## III. EXPERIMENTAL DETAILS

The x-ray absorption (NEXAFS) and resonant Auger experiments were performed at the SuperESCA beamline of the ELETTRA synchrotron radiation source in Trieste (Italy), using a modified SX-700 monochromator with a flux of the order of $10^{12}$ photons per second at a resolution of 5000. The experimental station consisted of an ultrahigh-vacuum chamber equipped with a spherical sector electron analyzer (VSW CLASS 150, 16-channel detector), LEED, standard excitation sources (electrons, x ray, UV), sample preparation facilities, and sample preparation chamber. NEXAFS was measured by collecting secondary electrons with a partial yield detector with the cutoff set to 200 eV. For the NEXAFS and the autoionization measurements of physisorbed $N_2$ on Xe/Ru(001), the photon bandwidth was set to about 50 meV. The resolution of the electron analyzer was also set to about 50 meV, using a pass energy of 5 eV. The sample was cooled by a homebuilt vertical cryostat working with liquid helium and reaching a temperature below 10 K, and cleaned and annealed by standard procedures. For preparing the $N_2$/Xe/Ru(001) layer system, the cleaned Ru sample was first exposed to 6 L (1 L$=10^{-6}$ Torr s) xenon and then heated up to 70 K to produce a dense Xe monolayer.[33] Subsequently a dilute $N_2$ monolayer was prepared by dosing 0.5 L $N_2$. All preparations were controlled with high-resolution XPS measurements.

## IV. RESULTS AND INTERPRETATION

### A. Excitation spectra and decay of on-resonance excitation

Figure 1 shows the vibrationally resolved excitation of the N 1$s$ core electron into the unoccupied $1\pi_g$ molecular orbital of a physisorbed $N_2$ monolayer on a Xe spacer monolayer on Ru(001). The NEXAFS spectrum is nearly identical to earlier $N_2$ gas-phase data at comparable resolution.[39] Because of the very weak surface bond, the electronic properties and with these the intramolecular bond of the neutral physisorbed $N_2$ molecule are essentially unchanged compared to the isolated $N_2$ molecule. An analysis of our data using Voigt profiles revealed an inherent Lorentzian linewidth of 132 meV that is equal to the lifetime linewidth of the $1\pi_g$ resonance of isolated $N_2$.[39] This corroborates that no additional decay channels are available to the $N_2$ physisorbate compared with isolated $N_2$, consistent with the location of the resonance below the Fermi level. Note that additional screening-induced inhomogeneous broadening is absent here, because the core-excited state is a neutral state.

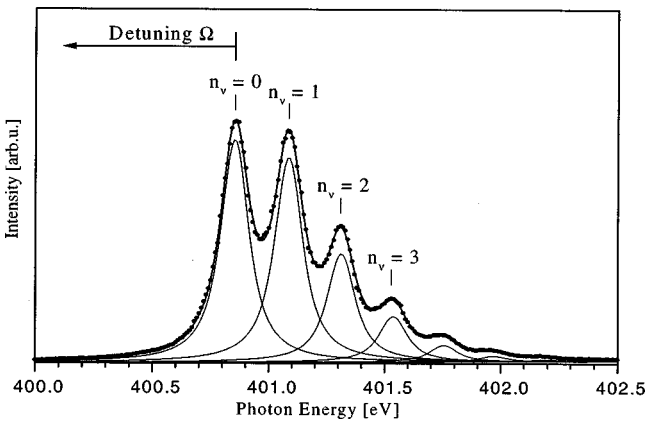


FIG. 1. Vibrationally resolved N $1s \rightarrow 1\pi_g$ photoabsorption of the physisorbed $N_2$ monolayer on a Xe spacer monolayer on a Ru(001) surface (photon bandwidth 50 meV).

The nuclear dynamics are studied for the resonant Auger process after resonant excitation on the low-energy side (to avoid vibrational interference) of the vibrational level $n_v = 0$ of the $1\pi_g$ resonance (the excitation always starts from the vibrational ground state). The detuning $\Omega$ of the excitation energy is defined to be zero on the maximum of the vibrational level $n_v = 0$ of the $1\pi_g$ resonance (photon energy is 400.86 eV) and to increase linearly with decreasing excitation energy.

In Fig. 2, the N 1$s$ autoionization spectrum of the physisorbed $N_2$ monolayer on a Xe spacer layer on Ru(001) is compared with the spectrum of isolated $N_2$ (Ref. 15) after excitation of the $1\pi_g$ resonance on the maximum of its vibrational level $n_v = 0$ ($\Omega = 0$). The very low direct photoemission contribution as deduced from off-resonance measurements has been subtracted from the spectrum. As for isolated $N_2$, autoionization of physisorbed $N_2$ takes place exclusively via the decay of the neutral core excitation. A charge transfer of the excited electron into the Ru metal, which is seen for example for molecularly chemisorbed $N_2$ (Ref. 40), is not possible because the $1\pi_g$ resonance of the physisorbed $N_2$ lies energetically below the Fermi level of the Ru substrate, as pointed out above.

Two clear differences between the autoionization spectra of isolated $N_2$ and of physisorbed $N_2$ are obvious immediately. The first concerns the linewidths. While in the spectrum of isolated $N_2$ the $3\sigma_g^{-1}$ participant transition can be vibrationally resolved, this participant transition is strongly broadened for physisorbed $N_2$ so that no vibrational fine structure can be observed. On the other hand, the linewidth of the $1\pi_u^{-1}$ participant transition is not too different from

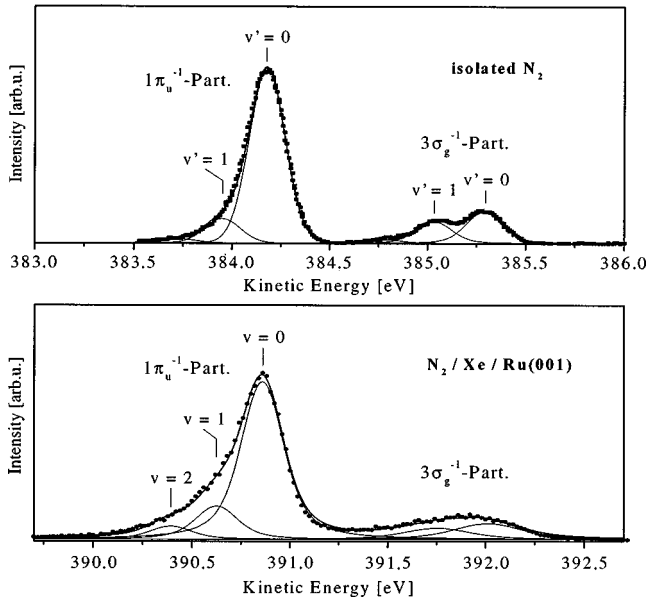


FIG. 2. N 1*s* autoionization spectrum of physisorbed $N_2$ on Xe/Ru(001) compared with the spectrum of isolated $N_2$ (Ref. 15) after excitation of the $1\pi_g$ resonance ($n_v=0$; 400.86 eV). The ranges of kinetic energies are different for the two cases because of final-state polarization screening for the adsorbate.

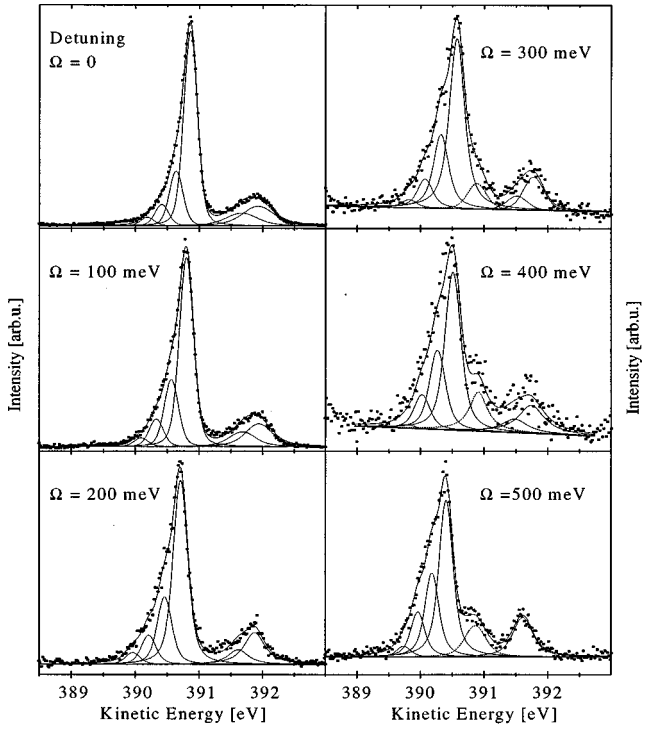


FIG. 3. Change of the vibrational structure of the $1\pi_u^{-1}$ (left) and $3\sigma_g^{-1}$ (right) participant transitions of physisorbed $N_2$ on Xe/Ru(001) caused by the detuning effect.

the isolated molecules, and the measured peak can be reproduced assuming (slightly changed, see below) vibrational contributions similar to the gas phase. The steepness of this line at the high kinetic-energy side can be fit well with Gaussians of about 240 meV; additional components of the same width for the higher vibrational excitations fit the entire peak well (also for the detuned spectra, see below). This Gaussian width is interpreted as due to the mentioned inhomogeneous broadening. Since this effect should be similar for both final states, we will assume such a Gaussian contribution also for the $3\sigma_g^{-1}$ line. The broadening in the latter line, fit with the assumption of three vibrational components (as suggested by the calculations for the isolated molecule, see below) is found to be about 460 meV, where its character—Gaussian or Lorentzian—is difficult to determine. We interpret the additional broadening as being due to the limited lifetime, or bandwidth, of the valence hole final state because of delocalization effects inside the physisorbed layer; it is seen that this contribution must be very different for the two final states. This is understandable from the smaller extension of the $1\pi_u$ orbitals compared to that of the $3\sigma_g$ orbitals so that the former overlap less in the physisorbed layer than the latter. Indeed the bandwidths of these two states have been determined to amount to 0.4 eV $[3\sigma_g^{-1}]$ and below 0.1 eV $[1\pi_u^{-1}]$ by angle-resolved photoemission.[41] The latter value makes it understandable that no Lorentzian contribution is found here for the $1\pi_u^{-1}$ line.

The second significant difference of the two spectra in Fig. 2 results from the detailed line shape of the $1\pi_u^{-1}$ participant transition. The asymmetric overall shape is a result of the underlying vibrational fine structure of the $1\pi_u^{-1}$ valence hole final state, with a dominant vibrational ground state and weak higher vibrational states. The line corresponding to the $1\pi_u^{-1}$ participant transition of physisorbed $N_2$ is clearly more asymmetric than that of the corresponding transition of isolated $N_2$ and indeed the line-shape analysis indicates a changed vibrational fine structure induced by the interaction within the physisorbed $N_2$ monolayer. Our fit to the spectra indicates a change of the vibrational energy of the $1\pi_u^{-1}$ state to about 246 meV (isolated molecule: 236 meV), i.e., a slight strengthening of the intramolecular bond of the (polarization-screened) final-state ion by condensation. This implies also a slightly decreased bond length and concomitant change of the Franck-Condon factors: the stronger dissimilarity between the potential curves for intermediate and final state, compared to the isolated molecule (where the curves lie almost on top of each other—see Fig. 5—resulting in the weakness of higher vibrational states[16,23]), leads to an increase of the relative intensities of higher vibrational states and consequently to a more asymmetric overall line shape.

### B. Detuning effects

We now examine the effect of detuning for our adsorbate case. The line shape of the $1\pi_u^{-1}$ participant transition of physisorbed $N_2$ depends distinctly on the excitation energy (Fig. 3). The photon energy has been varied in steps of 100 meV at the low-energy side of the vibrational level $n_v=0$ of the $1\pi_g$ resonance, to avoid vibrational interference effects. The small direct photoemission background, as deduced from off-resonance measurements, has been subtracted from all resonant core-hole decay spectra; only the resonantly enhanced contributions are shown. While the asymmetry is small for excitation in the maximum of the vibrational level $n_v=0$ of the $1\pi_g$ resonance ($\Omega=0$), the low-energy side of the $1\pi_u^{-1}$ peak grows with decreasing excitation energy (increasing detuning $\Omega$), and the line shape gets more asymmet-

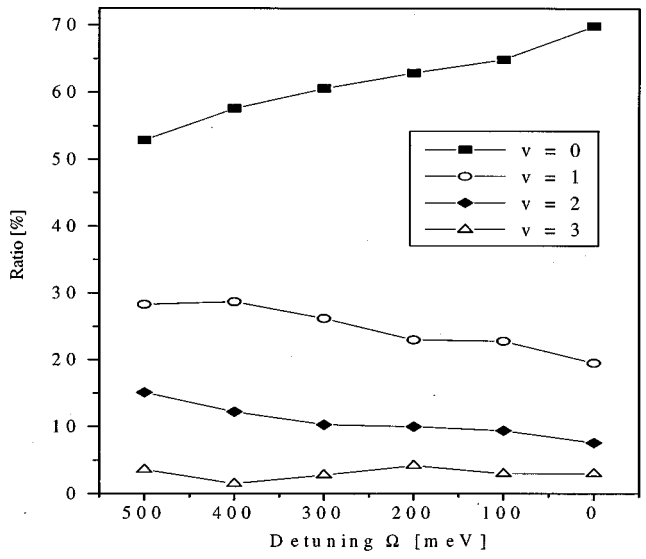


FIG. 4. Branching ratios of the individual vibrational final states of the $1\pi_u^{-1}$ participant transition (derived from their peak heights in the fitting curves) of physisorbed $N_2$ on Xe/Ru(001) as a function of detuning from the resonance.

ric. This implies that increasingly higher vibrational levels in the $1\pi_u^{-1}$ valence hole state are excited with increasing detuning $\Omega$ of the excitation energy. A fit of the vibrational fine structure for all individual decay spectra illustrates this trend. In Fig. 4, the branching ratios of the fitted vibrational levels of this final state, derived from the peak heights, are plotted versus the detuning $\Omega$. The vibrational ground state $v=0$ is dominant for excitation on the maximum of the vibrational level $n_v=0$ of the $1\pi_g$ resonance ($\Omega=0$), because the potential-energy surfaces of the $1\pi_g$ resonance and of the $1\pi_u^{-1}$ valence hole final state are still very similar, even in the adsorbate. Within the spectrum formation time $\tau_C$ (equal to the core-hole lifetime $\hbar/\Gamma$ for $\Omega=0$), the nuclear wave packet performs $\frac{1}{4}$ to $\frac{1}{2}$ of a vibrational period. Because of the sufficiently long propagation time in this case, the vibrational transition amplitudes are, to first order, proportional to the Franck-Condon factors between the vibrational nuclear wave functions of the $1\pi_g$ resonance and the $1\pi_u^{-1}$ valence hole states. The similarity of the potential-energy curves of these two states (Fig. 5) leads to the observed dominance of the $v=0$ peak for $n_v=0$ excitation. Detuning away from the maximum of the $1\pi_g$ resonance to lower excitation energies shortens $\tau_C$, as pointed out above. The shorter time available for propagation of the nuclear wave packet on the potential-energy surface of the $1\pi_g$ resonance state leads to the observed vibrational structure being increasingly determined by the Franck-Condon factors between the vibrational nuclear wave functions of the ground and the final valence hole states, until at large detuning a situation similar to direct photoemission is approached. Because the equilibrium nuclear distances of the ground and the $1\pi_u^{-1}$ valence hole states are quite different (Fig. 5), the excitation of higher vibrational levels in the $1\pi_u^{-1}$ valence hole state *increases* with increasing detuning below the $n_v=0$ resonance.[23] Examining the dispersion behavior (Fig. 6, lower half), we find the expected linear dispersion.[42] So the behavior of this final state is as expected.

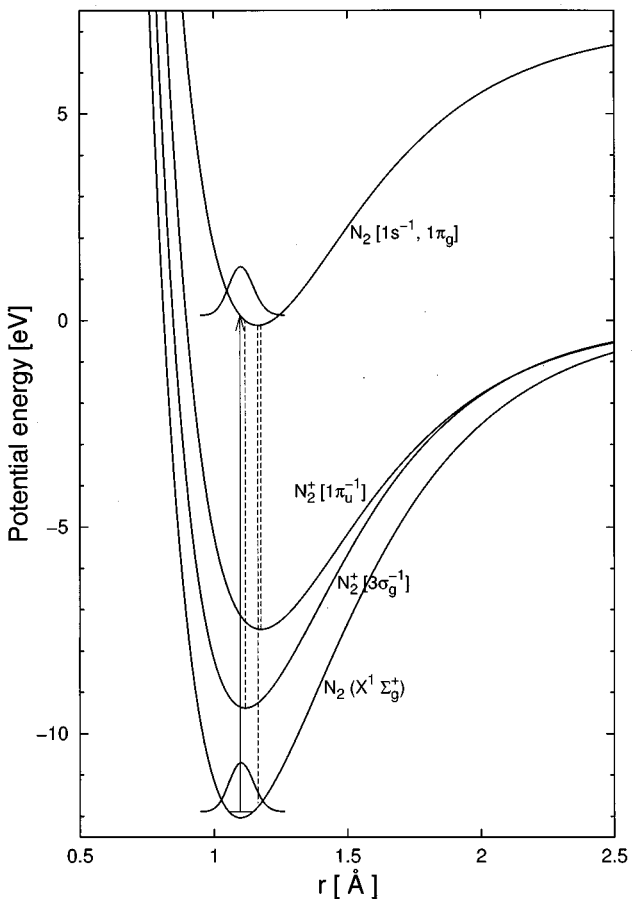


FIG. 5. Potential-energy curves for the relevant states of isolated $N_2$ (after Ref. 23). The individual curve shapes are correct to the eV scale indicated; their spacings are arbitrarily compressed. The dashed lines allow to compare the equilibrium bond lengths.

An additional peak at a *constant kinetic* energy of about 390.9 eV can be seen (Fig. 3, dashed) which is most clearly observed for a detuning $\Omega \geqslant 300$ meV; for higher photon energies (lower detuning) this peak is covered by the $1\pi_u^{-1}$ participant transition and at resonance coincides with it. Emission from radiation-induced dissociated fragments of $N_2$ as well as from Xe and the normal Auger emission from $N_2$ caused by higher orders of the synchrotron radiation can be excluded for energetic reasons and wrong behavior with detuning, respectively. Very recently this peak (and some weaker ones behaving similarly) has been seen for gas phase $N_2$ as well,[43] which also excludes a condensation effect. The appearance at constant kinetic energy independent of the detuning suggests an explanation based on the shape of the monochromator function. In accordance with Svensson and co-workers, we propose that this peak is induced by the tail of the monochromator function at the resonance excitation energy even under the detuned condition; in our case only the resulting strong peak stemming from the $1\pi_u^{-1}$ is seen. This explanation implies a much stronger tail of the monochromator function than expected from a Gaussian, as can be seen from its total absence in the calculations of Ref. 23 even for much broader Gaussian bandwidths. Simulations with various line shapes[44] show that very small contributions of broader radiation can produce these ''resonant ghosts'' (see

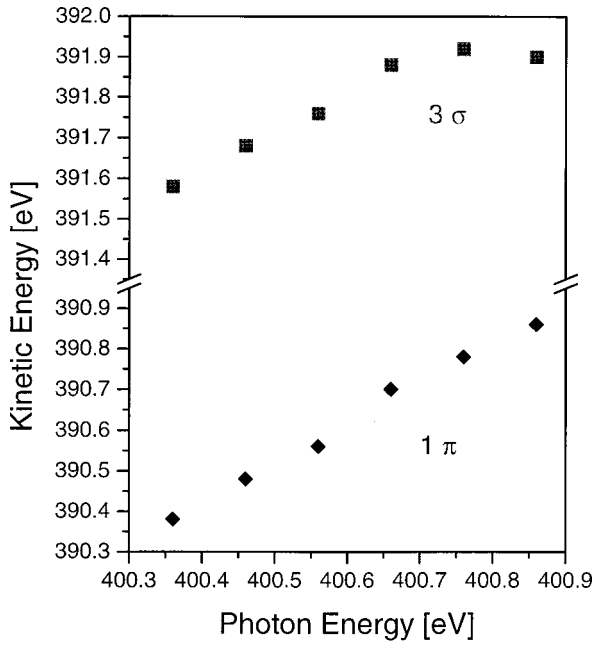


FIG. 6. Dispersion behavior of the $1\pi_u^{-1}$ and $3\sigma_g^{-1}$ participant decay peaks of physisorbed $N_2$ on Xe/Ru(001).

also below, Fig. 7), which compare well with the very recent gas-phase measurements mentioned.[43]

So the changes of the $1\pi_u^{-1}$ spectra with detuning can be understood. The behavior of the $3\sigma_g^{-1}$ final state does not conform to expectation, however. This can be seen from the upper half of Fig. 6, which shows that no linear dispersion is observed for its main maximum. For small detunings (up to about 0.2 eV), the position of the maximum stays essentially constant, but disregarding the first two points, linear dispersion is seen for higher detunings. On the other hand, persistence of the vibrational collapse with detuning, which is expected from calculations[23] and seen experimentally for the isolated molecule[16,43] and for the similar CO molecule,[14] is compatible with the measured line shape, which appears to sharpen for strong detuning (Fig. 3). The changed dispersion behavior can obviously not be due to a loss of coherence in the intermediate core-excited state as in cases of strong coupling to other degrees of freedom in this state,[34] because the latter is the same for the two final states, and because the intermediate-state electron is energetically localized and therefore cannot delocalize either into the substrate or into other condensate molecules (note that only the formation of the core hole pulls the $1\pi_g$ orbital below the Fermi level; on the neighboring $N_2$ molecules it lies above $E_F$ and is nonresonant with the localized exciton ''impurity'' state). Interestingly, a similar deviation from the expected linear dispersion has been found for the analogous $5\sigma^{-1}$ participant decay channel of a physisorbed CO monolayer on Xe/Ru(001).[45]

### C. Comparison with theoretical calculations

The question then arises whether the overall behavior of this peak can be understood by the combination of the final-state broadening already invoked as an explanation of the large width of this state (see above), with an effective shift induced in the broad peak maximum by the (now unresolved) vibrational collapse. We have therefore performed model calculations using the parameters of Ref. 23 for isolated $N_2$ (which are not fully adequate for our adsorbate case, see the discussion above), at the same time also examining the effect of the monochromator ghosts. Figure 7 shows the results, where the thin continuous lines are the spectra for sharp final states—i.e., modeling isolated $N_2$—excited with 50-meV bandwidth. The effect of resonant ghosts, in the form of an additional broad Lorentzian contribution of 10-eV width and 10% total intensity to the monochromator function selected to yield roughly the observed behavior, is also demonstrated; without this contribution, the dashed curves are obtained (best visible for 500-meV detuning and indistinguishable otherwise). The thick continuous lines give the results including both final-state broadenings, homogeneous

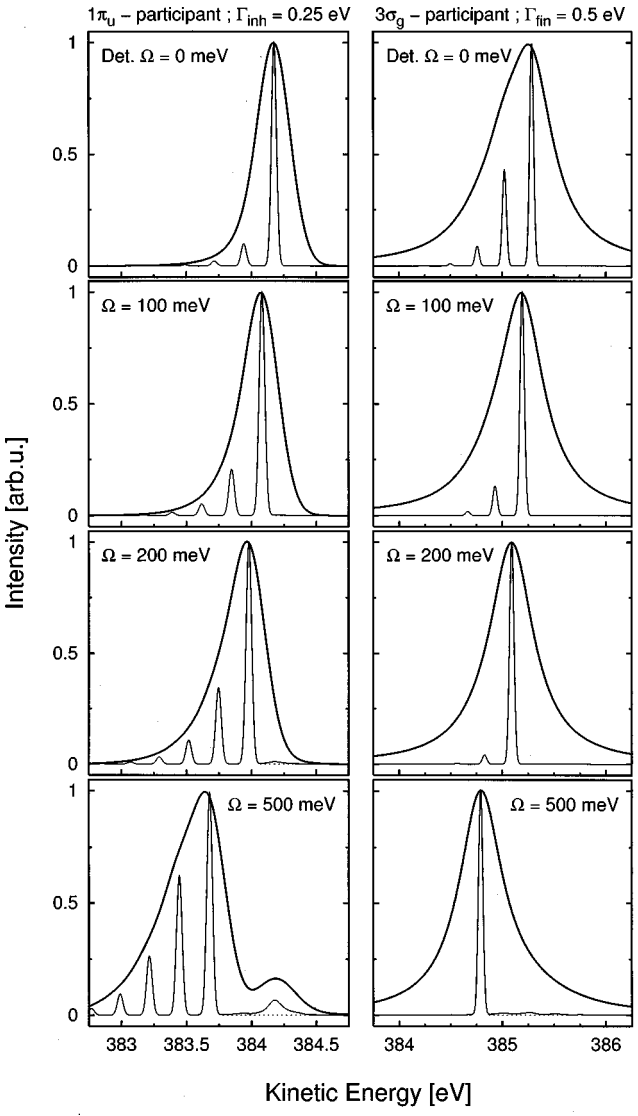


FIG. 7. Calculated vibrational structure of the $1\pi_u^{-1}$ (left) and $3\sigma_g^{-1}$ (right) participant transitions for the parameters of isolated $N_2$ used in Ref. 23. The thin continuous lines are the results for sharp final states, including a ''monochromator ghost'' contribution (see text; the dotted lines show the spectra without this contribution). The fat continuous lines are the results for final-state–broadened spectra as indicated on top [inhomogeneous Gaussian broadening by 0.25 eV for $1\pi_u^{-1}$ (left), and lifetime broadening with a Lorentzian of 0.5 eV for $3\sigma_g^{-1}$], including the same ghost contributions.

and inhomogeneous. For these, the sharp spectra including the monochromator ghosts have been convoluted with a Gaussian of width 0.25 eV of $1\pi_u^{-1}$ (assuming predominance of inhomogeneous broadening), and with a Lorentzian of width 0.5 eV for $3\sigma_g^{-1}$ (assuming predominance of the final-state delocalization). The unbroadened spectra, derived from the treatment of Ref. 23, are in fact in *very* good agreement with the mentioned very recent measurements on gas phase $N_2$,[43] in terms of the relative strengths of the vibrational components and their detuning behavior; this indicates the correctness of the used potential-energy curves. Compared to the present adsorbate measurements, the agreement is rather poor, again indicating changes of, in particular, the final-state potential curve. However, qualitatively the behavior is indeed as seen experimentally in this respect. For the $1\pi_u^{-1}$ peak (left-hand side), detuning turns on the higher vibrational excitations, and the broadened spectra consequently show a shape change similar to that seen experimentally; the dispersion is roughly linear as expected (in fact it is slightly stronger than linear because of the strong contributions of higher vibrations). For the broadened $3\sigma_g^{-1}$ peak the disappearance of higher vibrations by detuning is as expected; it slightly weakens the shift of the main peak for small detuning over a smaller range of detuning than in experiment (compare the shifts of the maxima between the unbroadened and the broadened spectra). For higher detunings, normal dispersion reappears.

So some of the unusual detuning behavior of the $3\sigma_g^{-1}$ peak is reproduced, but at a much smaller magnitude. Therefore, we cannot exclude that some additional physical effect might be operative in the dispersion behavior of the $3\sigma_g^{-1}$ peak, even though the vibrational collapse and the large final-state broadening do conspire to produce a qualitatively similar change. Such additional effects could be a complicated variation of the final density of states with energy whose coupling to the intermediate state would have to change with detuning; this might include possible changes of the internal vibrational structure through the band, which in connection with the change in evolution of the nuclear wave-packet upon detuning could then lead to a selection of certain final states. Another possibility would be that condensation increases the interference of resonant and direct photoemission (which here was assumed to be negligible and in fact is not contained at all in the calculations), which could be caused by angular effects. One possibility to check for such influences would be to investigate whether this behavior occurs only in molecular adsorbates such as $N_2$ and CO, or whether it is also present in broadened levels of atomic adsorbates. Measurements on the behavior of participant final states for rare-gas adsorbates would be very helpful in this respect; such measurements are planned.

## V. SUMMARY AND CONCLUSIONS

In conclusion, we have shown that even for physisorbed molecular systems, nuclear dynamical effects during resonant core-hole decay, as known for isolated molecules, can be detected. In the case of $N_2$, these are more easily observed for the $1\pi_u^{-1}$ than for the $3\sigma_g^{-1}$ final state because of the considerably larger bandwidth of the latter. When the excitation energy is detuned away from the maximum of the vibrational level $n_v=0$ of the N $1s\rightarrow 1\pi_g$ resonance to lower photon energies, the so-called detuning effect can be detected in the $1\pi_u^{-1}$ participant transition (turn-on of higher vibrational states) of a physisorbed $N_2$ monolayer on a Xe spacer layer on Ru(001), and likely persists in the $3\sigma_g$ final state (vibrational collapse) as well. The vibrational structure of the $1\pi_u^{-1}$ participant transition, which is changed noticeably compared to isolated $N_2$—probably because of polarization screening effects for the ionic final state within the $N_2$ physisorbate—depends on the excitation energy. Model calculations of the behavior of the changing vibrational structure with detuning for isolated $N_2$,[23] which reproduce very recent gas-phase measurements[43] very well, are in reasonable agreement with the adsorbate measurements after suitable broadening. The quantitative differences are understandable in terms of the influence of the environment. As a result of the persisting resonant Auger Raman effect, linear dispersion of the kinetic energy of the $1\pi_u^{-1}$ participant with excitation energy is observed. In contrast, the participant transition to the outermost valence state, the $3\sigma_g$ orbital, does not disperse as expected for small detunings. We have made it plausible that at least part of this behavior is due to the combination of the strong final-state broadening for this state with its persistent vibrational collapse, but since the calculations indicate a much smaller effect, additional contributions from other mechanisms cannot be excluded. A ''ghost'' peak has been observed under detuning conditions which can be attributed to deviations of the monochromator function from a Gaussian.

## ACKNOWLEDGMENTS

We thank S. Svensson and M. N. Piancastelli for valuable discussions and for information about their very recent measurements. The technical support of D. Cocco and M. Barnaba during data acquisition is gratefully acknowledged. Financial support of this project by the Deutsche Forschungsgemeinschaft under Project No. Me266/22-1, by the EC through its Large Scale Installation program ERBFMGETCT950022, and in part by a research grant to Z.W.G. from the Natural Sciences and Engineering Research Council (NSERC) of Canada, is gratefully acknowledged.

[1] T. Åberg, Phys. Scr. **41**, 71 (1992).

[2] T. Åberg and B. Crasemann, in *Resonant Anomalous X-Ray Scattering*, edited by G. Materlik, C. J. Sparks, and K. Fischer (North-Holland, Amsterdam, 1994), p. 431, and references therein.

[3] G. B. Armen and H. Wang, Phys. Rev. A **51**, 1241 (1995).

[4] E. Kukk, H. Aksela, S. Aksela, F. Gel'mukhanov, H. Ågren, and S. Svensson, Phys. Rev. A **53**, 3271 (1996).

[5] G. B. Armen, T. Åberg, J. C. Levin, B. Crasemann, M. H. Chen, G. E. Ice, and G. S. Brown, Phys. Rev. Lett. **54**, 1142 (1985).

[6] G. S. Brown, M. H. Chen, B. Crasemann, and G. E. Ice, Phys. Rev. Lett. **45**, 1937 (1980).

[7] A. Kivimäki, N. Naves de Brito, S. Aksela, H. Aksela, O.-P. Sairanen, A. Ausmees, S. J. Osborne, L. D. Dantas, and S. Svensson, Phys. Rev. Lett. **71**, 4307 (1993).
[8] H. Aksela, S. Aksela, O.-P. Sairanen, A. Kivimäki, N. Naves de Brito, and E. Nõmmiste, Phys. Rev. A **49**, R4269 (1994).
[9] H. Aksela, O.-P. Sairanen, A. Kivimäki, N. Naves de Brito, E. Nõmmiste, J. Tulkki, A. Ausmees, S. J. Osborne, and S. Svensson, Phys. Rev. A **51**, 1291 (1995).
[10] A. Flores-Riveros, N. Correia, H. Ågren, L. Pettersson, M. Bäckström, and J. Nordgren, J. Chem. Phys. **83**, 2053 (1985).
[11] N. Correia, A. Flores-Riveros, H. Ågren, K. Helenelund, L. Asplund, and U. Gelius, J. Chem. Phys. **83**, 2035 (1985).
[12] S. J. Osborne, A. Ausmees, S. Svensson, A. Kivimäki, O.-P. Sairanen, A. Naves de Brito, and H. Aksela, J. Chem. Phys. **102**, 7317 (1995).
[13] M. N. Piancastelli, M. Neeb, A. Kivimäki, B. Kempgens, H. M. Köppe, K. Maier, and A. M. Bradshaw, Phys. Rev. Lett. **77**, 4302 (1996).
[14] S. Sundin, F. Gel'mukhanov, H. Ågren, S. Osborne, A. Kikas, O. Björneholm, A. Ausmees, and S. Svensson, Phys. Rev. Lett. **79**, 1451 (1997).
[15] M. Neeb, J.-E. Rubensson, M. Biermann, and W. Eberhardt, J. Electron Spectrosc. Relat. Phenom. **67**, 261 (1994).
[16] M. N. Piancastelli, A. Kivimäki, B. Kempgens, M. Neeb, K. Maier, U. Hergenhahn, A. Rüdel, and A. M. Bradshaw, J. Electron Spectrosc. Relat. Phenom. **98-99**, 111 (1999).
[17] E. Kukk, H. Aksela, S. Aksela, F. Gel'mukhanov, H. Ågren, and S. Svensson, Phys. Rev. Lett. **76**, 3100 (1996).
[18] O. Björneholm, S. Sundin, S. Svenson, R. R. T. Marinho, A. Naves de Brito, F. Gel'mukhanov, and H. Ågren, Phys. Rev. Lett. **79**, 3150 (1997).
[19] F. Gel'mukhanov and H. Ågren, Phys. Rev. A **54**, 3960 (1996).
[20] L. S. Cederbaum and F. Tarantelli, J. Chem. Phys. **98**, 9691 (1993).
[21] Z. W. Gortel and J.-P. de Villiers, Chem. Phys. Lett. **245**, 41 (1995).
[22] E. Pahl, H.-D. Meyer, and L. S. Cederbaum, Z. Phys. D: At., Mol. Clusters **38**, 215 (1996).
[23] Z. W. Gortel, R. Teshima, and D. Menzel, Phys. Rev. A **58**, 1225 (1998).
[24] P. Skytt, P. Glans, J. Guo, K. Gunnelin, C. Såthe, J. Nordgren, F. Gel'mukhanov, A. Cesar, and H. Ågren, Phys. Rev. Lett. **77**, 5035 (1996).
[25] A. Cesar, F. Gel'mukhanov, Y. Luo, H. Ågren, P. Skytt, P. Glans, J. Guo, K. Gunnelin, and J. Nordgren, J. Chem. Phys. **106**, 3439 (1997).
[26] F. Gel'mukhanov, T. Privalov, and H. Ågren, Phys. Rev. A **56**, 256 (1997).
[27] P. F. Williams and D. L. Rousseau, Phys. Rev. Lett. **30**, 961 (1973).
[28] P. F. Williams, D. L. Rousseau, and S. H. Dworetsky, Phys. Rev. Lett. **32**, 196 (1974).
[29] O. Karis, A. Nilsson, M. Weinelt, T. Wiell, C. Puglia, N. Wassdahl, and N. Mårtensson, Phys. Rev. Lett. **76**, 1380 (1996).
[30] W. Wurth, Appl. Phys. A: Mater. Sci. Process. **65**, 155 (1997); **65**, 597 (1997).
[31] C. Keller, M. Stichler, G. Comelli, F. Esch, S. Lizzit, D. Menzel, and W. Wurth, Phys. Rev. B **57**, 11 951 (1998).
[32] C. Keller, M. Stichler, G. Comelli, F. Esch, S. Lizzit, D. Menzel, and W. Wurth, J. Electron Spectrosc. Relat. Phenom. **93**, 135 (1998).
[33] U. Höfer, M. J. Breitschafter, and E. Umbach, Phys. Rev. Lett. **64**, 3050 (1990).
[34] C. Keller, M. Stichler, G. Comelli, F. Esch, S. Lizzit, W. Wurth, and D. Menzel, Phys. Rev. Lett. **80**, 1774 (1998).
[35] N. V. Richardson and A. M. Bradshaw, in *Electron Spectroscopy—Theory, Techniques, and Applications*, edited by C. R. Brundle and A. P. Baker (Academic, New York, 1981), Vol. 4.
[36] E. W. Plummer and W. Eberhardt, Adv. Chem. Phys. **49**, 533 (1982).
[37] D. Schmeisser, F. Greuter, E. W. Plummer, and H.-J. Freund, Phys. Rev. Lett. **54**, 2095 (1985).
[38] W. Wurth (unpublished results).
[39] C. T. Chen, Y. Ma, and F. Sette, Phys. Rev. A **40**, 6737 (1989).
[40] C. Keller, M. Stichler, G. Comelli, F. Esch, S. Lizzit, W. Wurth, and D. Menzel (unpublished).
[41] M. Bertolo, W. Hansen, and K. Jacobi, Phys. Rev. Lett. **67**, 1898 (1991).
[42] Actually only the individual vibrational levels are expected to disperse linearly with photon energy, which is corroborated by examining the peaks obtained by our fits. However, in the present case the overall envelope shows essentially the same dispersion behavior because the peak maximum is determined by the $v=0$ line throughout.
[43] S. Svensson and M. N. Piancastelli (private communication).
[44] Z. W. Gortel (unpublished results).
[45] C. Keller, Ph.D. thesis, TU München, 1998.